JOURNAL OF AGRICULTURAL AND FOOD CHEMISTRY

pubs.acs.org/JAFC Article

Whole-Cell Biosensors Aid Exploration of Vanillin Transmembrane Transport

Xuanxuan Zhang,[#] Yang He,[#] Zhe Wu, Guoxia Liu, Yong Tao, Jian-Ming Jin,* Wei Chen,* and Shuang-Yan Tang*

Cite This: *J. Agric. Food Chem.* 2021, 69, 3114−3123 Read Online

ACCESS | Metrics & More | Article Recommendations | Supporting Information

ABSTRACT: Transcriptional regulatory protein (TRP)-based whole-cell biosensors are widely used nowadays. Here, they were demonstrated to have great potential application in screening cell efflux and influx pumps for small molecules. First, a vanillin whole-cell biosensor was developed by altering the specificity of a TRP, VanR, and strains with improved vanillin productions that were selected from a random genome mutagenesis library by using this biosensor as a high-throughput screening tool. A high intracellular vanillin concentration was found to accumulate due to the inactivation of the AcrA protein, indicating the involvement of this protein in vanillin efflux. Then, the application of this biosensor was extended to explore efflux and influx pumps, combined with directed genome evolution. Elevated intracellular vanillin levels resulting from efflux pump inactivation or influx pump overexpression could be rapidly detected by the whole-cell biosensor, markedly facilitating the identification of genome targets related to small-molecule transmembrane transport, which is of great importance in metabolic engineering.

KEYWORDS: *transcriptional regulatory protein, whole-cell biosensor, directed genome evolution, transmembrane transport, vanillin*

INTRODUCTION

Natural product whole-cell biosensors are the most efficient high-throughput screening tools due to their easy adaptation to fluorescence or color assays.[1] Transcriptional regulatory protein (TRP)-based whole-cell biosensors are effective in screening natural product hyper-producing strains.[2] However, the lack of innate transcription factors that respond to natural products of interest, especially those from plants, has limited TRP-based whole-cell biosensor application. Thus, TRP effector specificities should be engineered to respond to compounds other than their natural inducers.[3] These customized TRP-based whole-cell biosensors are powerful tools for screening highly efficient cell factories that produce targeted natural products.[4−6] In this study, we introduced another important biosensor function—identifying the microbial genomic targets involved in natural product transportation.

Metabolic engineering of cell factories to synthesize natural products has been widely studied.[7−9] In addition to heterologous biosynthetic enzymes, the metabolic network of host cells plays important roles in biosynthesis, such as contributing precursors, cofactors, energy, and transporters.[10−13] Thus, extensive optimization is required to efficiently direct intracellular resources to product formation. Apart from numerous targeted metabolic engineering strategies, directed genome evolution has marked potential in cell factory engineering since many genomic targets indirectly affect biosynthesis. However, these genomic targets are not easily predicted. Directed genome evolution allows the screening of unknown targets beneficial for biosynthesis on a genome-wide scale. Further, decoding the mechanism of action of these identified targets will clarify the functions of the metabolic network.[1] Similar to directed protein evolution, directed genome evolution involves genome mutagenesis library construction and high-throughput screening for improved product formation. With the development of various genome-editing tools, technologies for genome mutagenesis library construction are now available.[14] Realizing the high-throughput screening of hyper-producing cells has become a bottleneck in directed genome evolution.

Vanillin is one of the most widely used flavors in food and personal care products owing to its unique fragrance and antimicrobial and antioxidant activities.[15] Natural vanillin from vanilla pod extracts cannot meet the increasing demand.[16] Synthetic vanillin derived from biotechnological processes has become increasingly attractive since it can be regarded as a natural product.[17] Vanillin biosynthesis using ferulic acid as a substrate has been widely studied.[18−20] Ferulic acid is first activated to form an acyl intermediate through a feruloyl-CoA synthetase (Fcs), following which the CoA thioester is subsequently hydrated and converted to vanillin and acetyl-CoA by feruloyl-CoA hydratase/aldolase (Ech) (Figure 1A).[21] Several targeted metabolic engineering strategies, such as dynamic control and cofactor regeneration, have been used to optimize vanillin production.[22,23] Since this biosynthetic pathway involves cofactor and energy consumption *in vivo*, a genome-wide screening of targets related to biosynthetic efficiency is necessary.

Received: December 16, 2020
Revised: February 15, 2021
Accepted: February 22, 2021
Published: March 5, 2021

https://dx.doi.org/10.1021/acs.jafc.0c07886
J. Agric. Food Chem. 2021, 69, 3114−3123

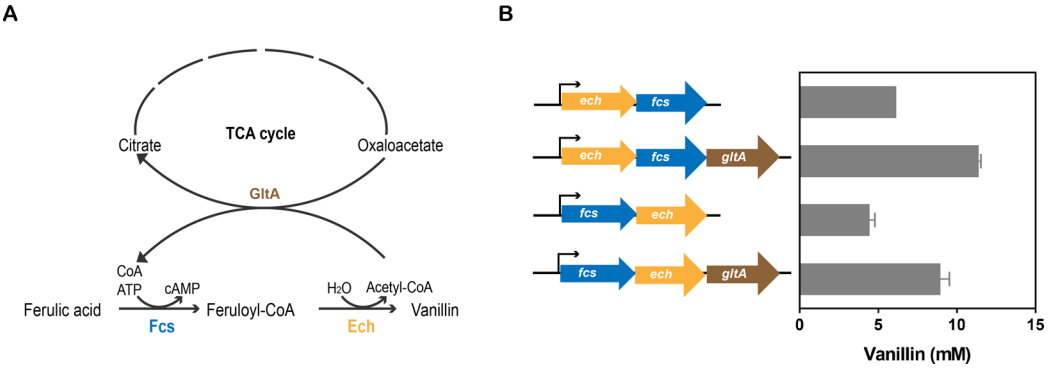

Figure 1. Construction and optimization of the vanillin biosynthetic pathway. (A) Diagram showing the vanillin biosynthetic pathway and regeneration of coenzyme A (CoA) from acetyl-CoA via the citric acid cycle. (B) Optimization of the biosynthetic pathway for improved vanillin production. Strain BW25113 expressing the vanillin biosynthetic pathway was grown at 37 °C for 2 h and then at 30 °C for 5 h after the addition of 1 mM L-arabinose. The media was supplemented with 20 mM ferulic acid, and the cells were grown for another 15 h at 30 °C. The data shown are from three replicate experiments and are expressed as the mean ± SD.

In this study, a high-quality vanillin whole-cell biosensor was developed by altering the specificity of VanR, a TRP obtained from *Corynebacterium glutamicum*.[24] Combined with directed genome evolution, we used the biosensor to identify several novel genomic targets related to vanillin biosynthesis. Interestingly, we observed that whole-cell biosensors were useful for screening potential efflux and influx pump proteins for natural products, which should enable subsequent studies of transmembrane transportation.

MATERIAL AND METHODS

General. Restriction enzymes, T4 DNA ligase, and DNA polymerases were purchased from Takara Bio Inc. (Dalian, China). Oligonucleotides were synthesized by Synbio Tech (Suzhou, China). Ferulic acid, vanillin, vanillic acid, and vanillyl alcohol were purchased from Sigma-Aldrich (St. Louis, USA).

The screening of transposon insertion library was performed in the yeast extract M9Y medium (M9 minimal salts, 1% (w/v) glucose, 2 mM $MgSO_4$, and 0.1 mM $CaCl_2$ supplemented with 0.1% (w/v) of yeast extract), while other cultures were done in a Luria−Bertani (LB) medium if not specially indicated. The antibiotics ampicillin (100 μg mL^{-1}), kanamycin (50 μg mL^{-1}), gentamicin (25 μg mL^{-1}), streptomycin (10 μg mL^{-1}), and chloramphenicol (25 μg mL^{-1}) were used when necessary.

Plasmid Construction. All plasmids, strains and primers used in this study are listed in Tables S2 and S3, respectively.

1) pV3-4-lacZ. The *lacZ* gene was amplified from the genomic DNA of strain MG1655 with primers *lacZ*-*Nco*I-fwd and *lacZ*-*Bgl*II-rev and ligated into plasmid pVanR[5] carrying gene encoding the VanR mutant V3-4 after digestion with *Nco*I and *Bgl*II.
2) pAH156-V3-4-lacZ. The fragment containing P_{vanABK}-*lacZ* and gene encoding the V3-4 mutant of VanR was amplified with primers pAH156-P_{vanABK}-*Sac*II-fwd and pAH156-vanR-*Sal*I-rev using plasmid pV3-4-lacZ as the template. The fragment was ligated into CRIM plasmid pAH156[25] after digestion with *Sac*II and *Sal*I.
3) pBAD-EFG, pBAD-FEG, pBAD-EF, and pBAD-EFG. Using the genomic DNA of *Pseudomonas syringae* as a template, the vanillin pathway genes *fcs* (GenBank accession no.ALU60828) and *ech* (GenBank accession no. ALU59956.1) were amplified with primer sets *fcs*-fwd-1/*fcs*-rev-1 or *fcs*-fwd-2/*fcs*-rev-2 and *ech*-fwd-1/*ech*-rev-1 or *ech*-fwd-2/*ech*-rev-2, respectively. The citrate synthase gene *gltA* encoding citrate synthase was amplified with primer set *gltA*-fwd-1/*gltA*-rev or *gltA*-fwd-2/*gltA*-rev using the genomic DNA of *Escherichia coli* MG1655 as a template. To get the vector fragment, PCR was performed using plasmid pFA[5] as a template with primers pFA-fwd and pFA-rev. Fragments containing genes *ech1*, *fcs1*, and *gltA1* and the vector fragment were assembled, resulting in plasmid pBAD-EFG. Fragments containing genes *fcs2*, *ech2*, and *gltA2* and the vector fragment were assembled, resulting in plasmid pBAD-FEG. Using plasmid pBAD-EFG and pBAD-FEG as a template, PCR amplifications were performed with primer sets pBAD-vector-*Sac*I-fwd /EF-pBAD-*Sac*I-rev and pBAD-vector-*Sac*I-fwd/FE-pBAD-*Sac*I-rev; after the PCR, products were digested with *Sac*I and then self-ligated, resulting in plasmids pBAD-EF and pBAD-FE, respectively.
4) pS95s-acrA. The *acrA* gene was amplified from the genomic DNA of strain MG1655 with primers *acrA*-fwd and *acrA*-rev and ligated into plasmid pS95s.[26]

Construction of the VanR Library. The site-saturation mutagenesis library of *vanR* was constructed by overlap extension PCR.[27] Using *vanR*1-fwd/*vanR*1-rev and *vanR*2-fwd/*vanR*2-rev as two sets of primers, two fragments containing the site-saturation mutagenesis at positions 103, 143, and 168 of the *vanR* gene were amplified with plasmid pVanR as a template. Equimolar aliquots of the two amplified fragments (2 nmol each) were PCR assembled. The PCR product was used as the megaprimers to perform the MEGAWHOP PCR[28] using pVanR as a template. Then, *Dpn*I (20 U) digestion was performed at 37 °C for 12 h, after which *Dpn*I was inactivated at 80 °C for 20 min. Then, the PCR products were transformed into the *E. coli* strain MC1061, and around 10^6 transformants were recovered. Ten clones were randomly picked and sequenced, and mutations at the indicated positions were confirmed with no additional point mutations. All colonies from the agar plates were used for plasmid isolation to prepare the plasmid library.

VanR Library Screening. The VanR plasmid library was used to transform strain BW25113 (over 3×10^5 transformants were recovered). Fluorescence-activated cell sorting (FACS) was performed on a BD FACS Aria II flow cytometer (BD Biosciences, San Jose, USA). Fluorescence was excited at 561 nm, and emission was collected using a 610/20 nm band-pass filter. In the first round of negative screening, cells were precultured overnight in an LB medium and then diluted to OD_{600} = 0.2 in the same medium with 6 mM ferulic acid, 1 mM vanillic acid, and 1 mM vanillyl alcohol supplemented. The cells were then grown for 12 h, and the least fluorescent 2.4×10^5 cells were collected (representing 80% of all cells sorted). This was performed to eliminate VanR variants with high levels of leaky expression or responsive to ferulic acid, vanillic acid, or vanillyl alcohol. The collected cells were then induced with 3 mM vanillin and grown for 12 h and subjected to positive screening. The most fluorescent 3×10^3 cells were sorted from 3×10^5 cells. This dual screening was repeated three times followed by a final round of negative screening in the absence of an inducer. Five clones were selected for rescreening in test tubes in the presence of 0

https://dx.doi.org/10.1021/acs.jafc.0c07886
J. Agric. Food Chem. 2021, 69, 3114−3123

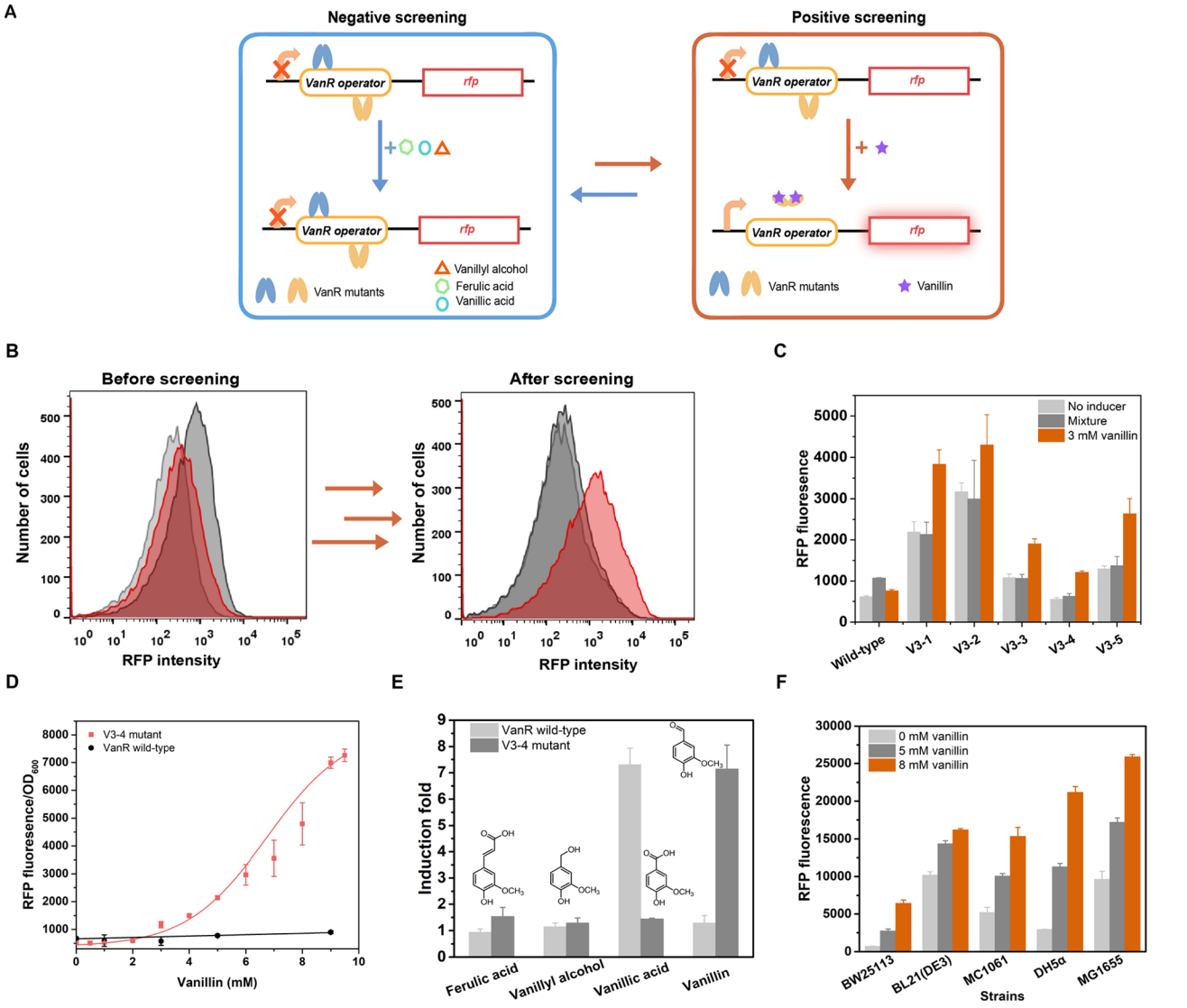

Figure 2. Construction and characterization of a vanillin-responsive VanR variant. (A) High-throughput screening strategy for directed evolution of VanR with altered specificity. (B) Flow cytometry analysis of RFP expression from the VanR saturation mutagenesis library before and after three rounds of dual screening. Cells were treated with 3 mM vanillin (red), a mixture containing 6 mM ferulic acid, 1 mM vanillic acid, and 1 mM vanillyl alcohol (dark gray), or no inducer (light gray). (C) RFP fluorescence of wild-type VanR and the VanR variants selected from the library after iterative FACS screening. Cells were treated with 3 mM vanillin (red), a mixture of 6 mM ferulic acid, 1 mM vanillic acid, and 1 mM vanillyl alcohol (dark gray), or no inducer (light gray). (D) RFP fluorescence (normalized to cell density) of strain BW25113 expressing the VanR variant V3-4 as a function of vanillin concentration. The dose−response curve of wild-type VanR is included for reference. (E) Induction fold of strain BW25113 expressing wild-type VanR or VanR variant V3-4 in response to 6 mM of the indicated compounds. (F) RFP fluorescence of the indicated *E. coli* strains expressing the VanR variant V3-4 in the absence or presence of different vanillin concentrations. The data shown are from three replicate experiments and are expressed as the mean ± SD.

mM, 3 mM vanillin, and a mixture containing 6 mM ferulic acid, 1 mM vanillic acid, and 1 mM vanillyl alcohol.

Molecular Docking. All protein structure figures were generated by the PyMOL program (http://www.pymol.org) using the crystal structure of VanR binding with vanillic acid (PDB code: 6LG2). The binding models of vanillin to the VanR mutants were calculated by Rosetta ligand docking,[29] and residues with a distance of 6 Å from the binding pocket were set as flexible during the docking procedure. Each docking cycle generate 500 binding models. The model with the lowest docking score was used as the final model.

RFP Fluorescence Assays. A single colony of strain BW25113 harboring plasmid pVanR was grown overnight in the LB medium at 37 °C and then diluted to OD_{600} = 0.01 in the same medium containing an appropriate concentration of vanillin, ferulic acid, vanillic acid, or vanillyl alcohol and allowed to grow under the inducing condition at 30 °C for 12 h. The OD_{600} and RFP fluorescence emission were measured with a SynergyMx multi-mode microplate reader (BioTek, Vermont, USA) (556 nm excitation filter and 586/20 nm emission filter).

Strain Construction. Using plasmid pAH156-V3-4-lacZ, the fragment containing the gene encoding VanR V3-4 variant and $P_{vanABK2}$-*lacZ* construct was integrated into the *E. coli* BW25113 chromosome using helper plasmid pAH69, as described,[25] resulting in strain V3-4. The integration was verified by PCR.

Genes *ptsH*, *acrA*, *lysC*, *slyB*, *yohG*, *mhpT*, *acrB*, *tolC*, *acrD*, *ompF*, and *ompC* in *E. coli* were individually replaced with a kanamycin cassette flanked by the FLP recognition target (FRT) site using a one-step inactivation method.[30] Then, the FRT-flanked *kan* gene was removed using flippase-mediated recombination, resulting in strains Δ*ptsH*, Δ*acrA*, Δ*lysC*, Δ*slyB*, Δ*yohG*, Δ*mhpT*, Δ*acrB*, Δ*tolC*, Δ*acrD*, Δ*ompF*, and Δ*ompC*.

***β*-Galactosidase Activity Assay.** *E. coli* strain V3-4 expressing the vanillin biosynthetic pathway was grown overnight in an LB medium at

https://dx.doi.org/10.1021/acs.jafc.0c07886
J. Agric. Food Chem. 2021, 69, 3114−3123

37 °C and then diluted to OD_{600} = 0.01 in the same medium. In the absence or presence of 0, 4, 6, 8, and 12 mM ferulic acid, the cells were further grown for 16 h at 30 °C. Cells were collected by centrifugation at 4 °C and resuspended in McIlvaine buffer (200 mM Na_2HPO_4, 100 mM citric acid, pH 6.0). After ultrasonication and centrifugation, the supernatant was used as a cell lysate. The β-galactosidase activity was determined by incubating 15 μL of crude enzyme extracts with 20 μL of 25 mM *o*NPG in McIlvaine buffer at 37 °C for 10 min, and the reaction was stopped by adding 150 μL of 1 mM Na_2CO_3. The increase in absorbance at 420 nm due to the release of *o*-nitrophenol (ONP) was measured. One unit (U) of enzyme activity was defined as the amount of enzyme required to liberate the equivalent of 1 μM ONP per minute under the assay conditions.

Construction and Screening of the Transposon Insertion Library. Strain V3-4 was transformed with plasmid pTn10[31] and plated on LB agar containing 1 mM IPTG. Then, around 20,000 colonies were collected, grown, and transformed with plasmid pBAD-EFG. The transformants were plated on M9Y agar containing 30 μg/mL X-Gal, 1 mM L-arabinose, and 10 mM ferulic acid. After incubation at 30 °C for 16 h, the darkest blue colonies (by the eye) were selected for quantifying vanillin production in the liquid culture.

Locations of transposon insertion in the chromosome were identified by thermal asymmetric interlaced TAIL-PCR performed as described.[1,32] Genomic DNA of strains exhibiting increased vanillin yields was used as a template.

Quantification of Vanillin Productions and Intracellular Vanillin Concentration. A colony of *E. coli* strain expressing the vanillin biosynthetic pathway was grown for 12 h at 37 °C and then diluted to OD_{600} = 0.01. After being further grown at 37 °C for 2 h, 1 mM L-arabinose was added, and the cells were grown at 30 °C for 5 h. Then, a total of 13.3 mM ferulic acid was supplemented five times at an interval of 1 h. After ferulic acid supplementation, the cells were further grown for 15 h at 30 °C. Then, 500 μL of the sample was harvested, and the same volume of ethanol was added and mixed. Then, the sample was filtered with a 0.2 μm membrane filter and analyzed by HPLC to detect vanillin production.

For intracellular vanillin measurement, 2.5 mL samples were collected by centrifugation. The supernatant was removed, and cells were washed twice with phosphate buffered saline (PBS). Then, the cells were resuspended in 500 μL of PBS and disrupted by sonication with a JY92-IIN Ultra Sonic Cell Crusher (Ningbo, China). After centrifugation, 10 μL of the supernatant was analyzed by HPLC, and the vanillin concentration was regarded as the intracellular vanillin concentration.

HPLC Quantification. HPLC was performed using a Shimadzu LC-20A system equipped with a photodiode array detector (Shimadzu Corp., Kyoto, Japan). A Waters Symmetry C18 column (250 × 4.6 mm, 5 μm) working at 30 °C was used for all analyses. Mobile phase A was 5% acetic acid, and B was methanol. A linear gradient of mobile phase B (0−20 min, increased from 30 to 50%) at a flow rate of 0.5 mL/min was used for separation. The compounds were monitored at 260 nm, and the concentrations were calculated from a standard curve prepared with authentic vanillin or ferulic acid.

RESULTS

Construction and Optimization of the Vanillin Biosynthetic Pathway in *E. coli*. A heterologous vanillin biosynthetic pathway was constructed in *E. coli* by co-expressing Fcs and Ech from *P. syringae* under the control of the P_{BAD} promoter (Figure 1A). Strain BW25113 expressing this operon (plasmid pBAD-EF) produced 6.066 ± 0.051 mM vanillin, and the yield was 30.33% (Figure 1B). The citrate synthase GltA, encoded by *gltA*, catalyzes the conversion of acetyl-CoA and oxaloacetic acid to form citrate and CoA. Importantly, this enzyme improves vanillin biosynthesis efficiency by accelerating intracellular CoA regeneration (Figure 1A).[23] Thus, we introduced GltA. As shown in Figure 1B, the effect of the order of gene *fcs* and *ech* in the operon on vanillin production was explored in the presence or absence of gene *gltA*. It was found that the operon containing gene *ech* upstream of gene *fcs* exhibited higher vanillin production. The operon in plasmid pBAD-EFG exhibited approximately 1.9-fold higher vanillin production than the operon lacking GltA (Figure 1B).

Development of a Vanillin-Specific VanR Variants. The *vanABK* operon is responsible for vanillic acid catabolism in *C. glutamicum*.[33] In the absence of vanillic acid, the TRP VanR binds to the operator sequence and represses *vanABK* operon transcription. When vanillic acid is present, it binds to the VanR protein, which releases it from the promoter following a conformational change, thus activating operon transcription.[24] We introduced the VanR/P_{vanABK}'-RFP reporter system into *E. coli*.[5]

To alter the effector specificity of VanR from vanillic acid to vanillin, amino acid residues Y103, R148, and Y168, which are located in the effector binding pocket, were chosen for simultaneous site-saturation mutagenesis (Figure S1). The mutagenesis library containing 3.0 × 10^5 transformants was subjected to screening by fluorescence-activated cell sorting (FACS). Positive screening was designed to enrich VanR mutants responsive to vanillin, while negative screening removed mutants with leaky expression levels or those responsive to ferulic acid, vanillic acid, and vanillyl alcohol (Figure 2A). Figure 2B depicts the red fluorescence protein (RFP) fluorescence in the library before and after three rounds of dual positive−negative screening. We selected five vanillin-responsive variants finally. The sequencing results revealed the amino acid substitutions in these mutants (Table 1). Among them, variant V3-4 exhibited the lowest basal expression and the largest fluorescence improvement in the presence of vanillin compared with that in the presence of ferulic acid, vanillic acid, and vanillyl alcohol (Figure 2C). Thus, this VanR mutant was used for downstream characterization. RFP fluorescence of strain BW25113 expressing variant V3-4 and wild-type VanR is compared in Figure 2D as a function of vanillin concentration. For variant V3-4, around 13.7-fold of fluorescence induction occurred in a range of 0−9.5 mM vanillin, and half-maximal induction response occurred at approximately 6.74 mM vanillin. The induction effects of substrate ferulic acid, the vanillin analog vanillyl alcohol, or the original VanR inducer vanillic acid on VanR wild type and variant V3-4 were determined compared with that of vanillin. As shown in Figure 2E, the VanR wild type and V3-4 variant showed specific responses toward vanillic acid and vanillin, respectively. Ferulic acid or vanillyl alcohol exhibited little induction effect on both VanR wild type and V3-4 variant. This induction specificity of variant V3-4 was very important for its use as a vanillin biosensor in downstream metabolic engineering tasks because both vanillic acid and vanillyl alcohol are major byproducts of vanillin biosynthesis.[34]

Table 1. Amino Acid Substitutions of the Selected VanR Variants

	amino acid positions		
VanR variants	103	148	168
Wild-type	Y	R	Y
V3-1	W	R	D
V3-2	F	R	I
V3-3	L	N	P
V3-4	E	I	T
V3-5	P	G	Q

https://dx.doi.org/10.1021/acs.jafc.0c07886
J. Agric. Food Chem. 2021, 69, 3114−3123

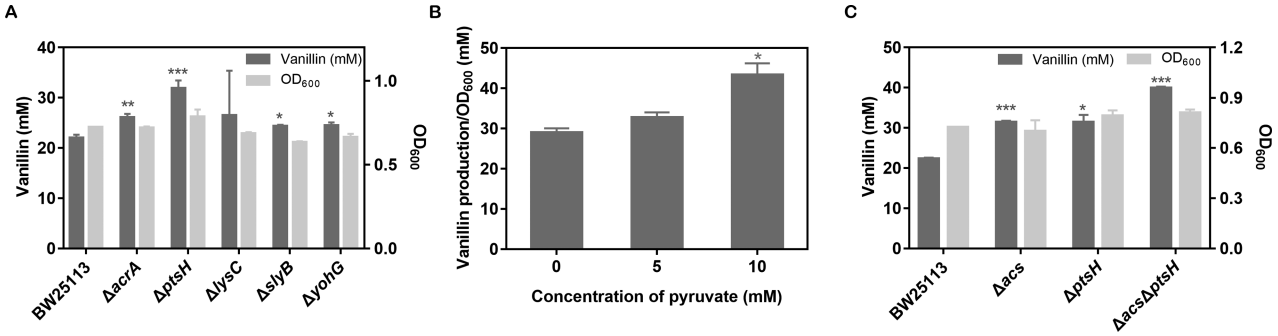

Figure 3. Application of vanillin whole-cell biosensors. (A) Vanillin production of five knockout mutant strains. The knocked-out genes were identified by directed genome evolution. (B) Effect of pyruvate supplementation on vanillin biosynthesis. (C) Vanillin production of strain BW25113 with the indicated genes knocked out. Here, 66.5 mM ferulic acid was used in the reactions. Two-tailed Student's *t* test was used for statistical analysis (*$P < 0.05$; **$P < 0.01$; ***$P < 0.001$).

Their presence significantly reduces the efficiency of vanillin biosynthesis and makes the downstream vanillin purification process more difficult. Furthermore, we determined the induction capability of the V3-4 variant in various *E. coli* strains. The results demonstrated that this regulatory system functioned in different strains. However, non-specific expression and the highest fluorescence induction were achieved in strain BW25113 (Figure 2F).

To explore the characteristics of VanR induction, we modeled the binding of vanillin to the selected variants. As depicted in Figure S1B−F, vanillin binds to the selected VanR variants at the same pocket as in the wild-type VanR. In variant V3-4, the Y103E mutation increased the specificity of VanR for vanillin by forming a hydrogen bond with it while being unfavorable for vanillic acid binding because of ionic repulsion. At the same time, the R148I mutation impaired the binding capacity for vanillic acid by removing the salt bridge between R148 and the carboxyl group of vanillic acid, which largely contributes to the binding of vanillic acid by wild-type VanR (Figure S1E).

Construction, Functional Validation, and Application of Vanillin Whole-Cell Biosensors. Strain V3-4 was constructed by integrating the constitutively expressed V3-4 variant and the $P_{vanABK2}$-*lacZ* construct into the strain BW25113 chromosome. *β*-Galactosidase was used as a reporter to facilitate high-throughput screening on agar plates. It was found that for strain V3-4 expressing the vanillin biosynthetic pathway cultured in the presence of ferulic acid, there was a positive correlation between *β*-galactosidase activity and vanillin production (Figure S2), indicating the feasibility of using the *β*-galactosidase reporter for high-throughput screening.

A random transposon insertion library was constructed in strain V3-4. To verify random transposon insertion, five colonies were randomly picked from the agar plates, and the gene targets disrupted by transposon were identified (Table S1). The results showed that the insertion of transposon was indeed random. The library strains were then transformed with plasmid pBAD-EFG to express the vanillin biosynthetic pathway. The transformants were grown on M9Y agar plates supplemented with L-arabinose, ferulic acid, and X-Gal. The blue color of the colonies, implicating the expression levels of *lacZ* gene, could be used to estimate intracellular vanillin biosynthesis and rapidly identify gene disruption that leads to increased vanillin production. We selected vanillin hyper-producers by choosing the clones with the most intense blue color. Since vanillin biosynthesis involves ATP hydrolysis, CoA circulation, and possible vanillin transportation,[35] the metabolic network of the host cell should be explored for the possibility of improving biosynthetic capability. Colonies showing the most intense blue color, which represented vanillin hyper-producing cells, were selected for rescreening using high-performance liquid chromatography (HPLC) to quantify vanillin production.

After screening ~3.0×10^5 library transformants, the five bluest clones with the most intense blue color were selected and assayed for vanillin production (Figure S3). These clones exhibited 10.8−45.1% improvement in vanillin biosynthesis compared with the wild-type V3-4 strain. Identification of the transposon insertion locations in the mutant strains revealed that *acrA*, *ptsH*, *lysC*, *slyB*, and *yohG* were disrupted (Figure S4). To confirm the functions of these targets, each gene was individually knocked out in strain BW25113, resulting in mutant strains Δ*acrA*, Δ*ptsH*, Δ*lysC*, Δ*slyB*, and Δ*yohG*. After transformation with plasmid pBAD-EFG, we confirmed their improved vanillin biosynthesis (Figure 3A and Figure S5A). Among the five mutant strains, the Δ*ptsH* strain produced ~1.5-fold more vanillin than the wild-type BW25113 strain. There was no additive effect found in the combination of deletions of *ptsH* and the other four genes selected (Figure S5B). Gene *ptsH* encodes a general component of the phosphoenolpyruvate-dependent phosphotransferase system (PTS). PTS consumes 50% of the available phosphoenolpyruvate (PEP) when the *E. coli* cells are grown in minimal medium using glucose as a carbon source.[36] PEP and pyruvate activate the conversion of acetyl-CoA to acetate by acetyl phosphate, which produces CoA and ATP (Figure S6).[37] Therefore, deleting *ptsH* increased intracellular PEP levels and accelerated CoA and ATP regeneration for vanillin biosynthesis. To confirm the mechanism, we investigated the effect of pyruvate supplementation on vanillin biosynthesis. Our results show that vanillin production (normalized to cell density) was improved with increasing pyruvate concentration (Figure 3B). Furthermore, acetyl-CoA synthetase (ACS) is responsible for the irreversible conversion of acetate to acetyl-CoA, which consumes ATP.[38] Thus, we knocked out the *acs* gene in the Δ*ptsH* strain to stabilize CoA and ATP regeneration. As expected, the double mutant strain exhibited a 1.85-fold improvement in vanillin biosynthesis (Figure 3C and Figure S5C).

VanR Whole-Cell Biosensor Aid in Vanillin Transmembrane Transportation Studies. Interestingly, the Δ*acrA* mutant yielded a vanillin concentration that was only slightly higher than that of the wild-type BW25113 strain (Figure 3A) even though the agar plate colony of this strain displayed the darkest blue color among all the mutant strains

https://dx.doi.org/10.1021/acs.jafc.0c07886
J. Agric. Food Chem. 2021, 69, 3114−3123

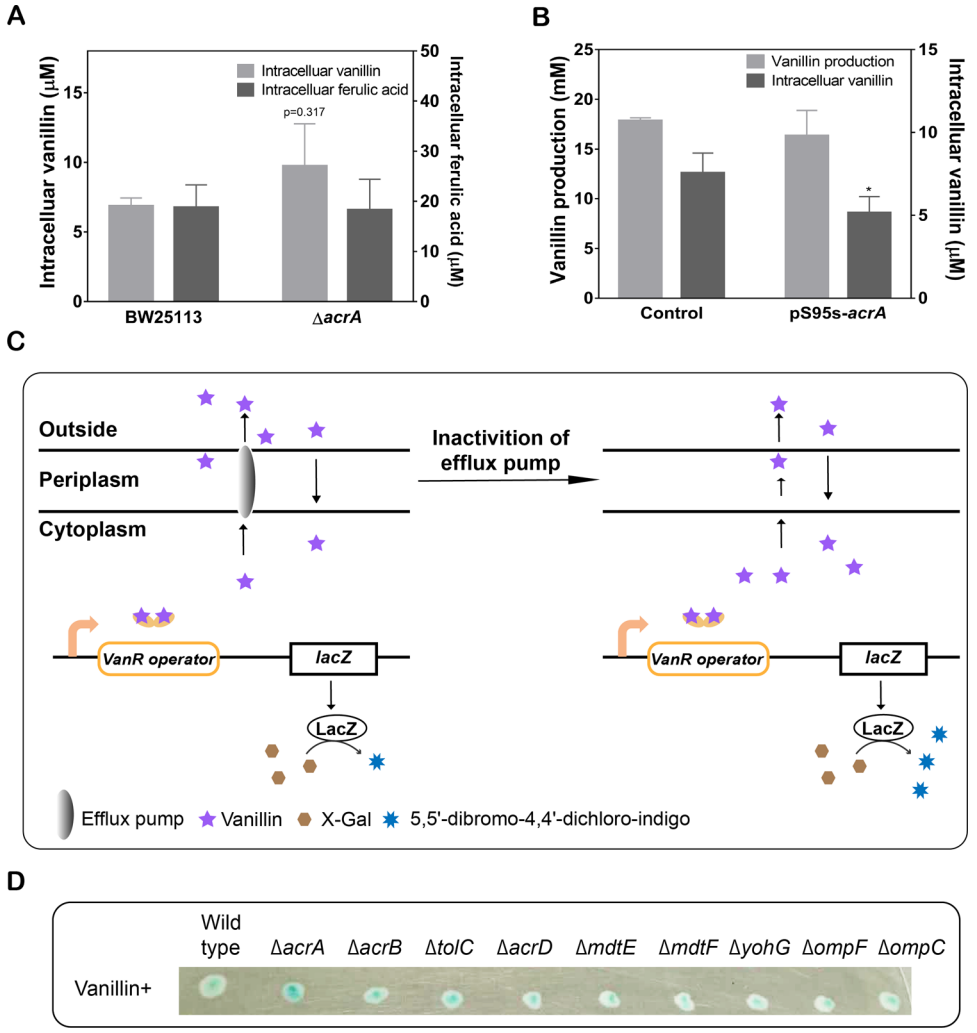

Figure 4. Whole-cell biosensor-aided efflux pump screening. (A) Intracellular vanillin and ferulic acid concentration in wild-type BW25113 and Δ*acrA* strains. (B) Vanillin production and intracellular vanillin concentration of strain BW25113 overexpressing AcrA (pS95s-acrA) or control vector. (C) Diagram showing the mechanism for biosensor-aided efflux pump screening. (D) Selected indicated strains were grown on agar plates supplemented with 3 mM vanillin and 30 μg/mL X-Gal. The data shown are from three replicate experiments and are expressed as the mean ± SD. Two-tailed Student's *t* test was used for statistical analysis (*$P < 0.05$).

(Figure S3). Periplasmic AcrA is a component of the *E. coli* AcrAB-TolC and AcrAD-TolC multidrug efflux pumps.[39] If vanillin is transported out of the cell by these pumps, then deleting *acrA* would impede vanillin efflux. Consequently, vanillin would accumulate within the cell, which can be monitored by the whole-cell biosensor. To verify this hypothesis, we evaluated the intracellular vanillin concentration when AcrA was inactivated or overexpressed. The same amount of cells were collected and resuspended in the same volume of PBS buffer. After cell lysis, the concentrations of vanillin and ferulic acid in the supernatant were determined. Inactivation of gene *acrA* increased the intracellular vanillin concentration, while the intracellular ferulic acid concentration only slightly changed (Figure 4A). In cells overexpressing AcrA, the total vanillin production decreased slightly due to the increased cell metabolic burden, but the intracellular vanillin concentration decreased significantly (Figure 4B), supporting that AcrA is involved in vanillin export.

The strategy of using whole-cell biosensors to screen for possible efflux pumps is depicted in Figure 4C. The intracellular vanillin concentration is elevated due to efflux pump dysfunction and can be easily detected by the whole-cell biosensor. We performed several experiments to validate this strategy. Since AcrAB/TolC, AcrAD/TolC, MdtEF/TolC, and YohG efflux pumps[39−42] confer *E. coli* resistance to various toxic compounds, *acrA*, *acrB*, *tolC*, *acrD*, *mdtE*, *mdtF*, *yohG*, and genes encoding two porins, *ompF* and *ompC*,[43] were individually knocked out in strain V3-4 to determine whether our whole-cell biosensor can identify vanillin efflux pumps. Among the mutant colonies, the Δ*acrA* strain showed the darkest blue color, indicating a markedly higher intracellular vanillin concentration due to deficient vanillin efflux (Figure 4D). The Δ*acrB* and Δ*tolC* strains displayed a lighter blue color than the Δ*acrA* strain, while the other strains showed a similar color as the wild-type strain.

We further explored the applicability of screening for a vanillin influx pump using this vanillin whole-cell biosensor. As depicted in Figure 5A, when a potential influx pump protein was overexpressed in the presence of extracellularly supplemented vanillin, the elevated intracellular vanillin concentration due to increased influx would be detected by the biosensor. To test the feasibility of this strategy, four reported influx pumps, MhpT, NanT, YgcS, and ActP, which transport 3-hydroxyphenylpropi-

https://dx.doi.org/10.1021/acs.jafc.0c07886
J. Agric. Food Chem. 2021, 69, 3114−3123

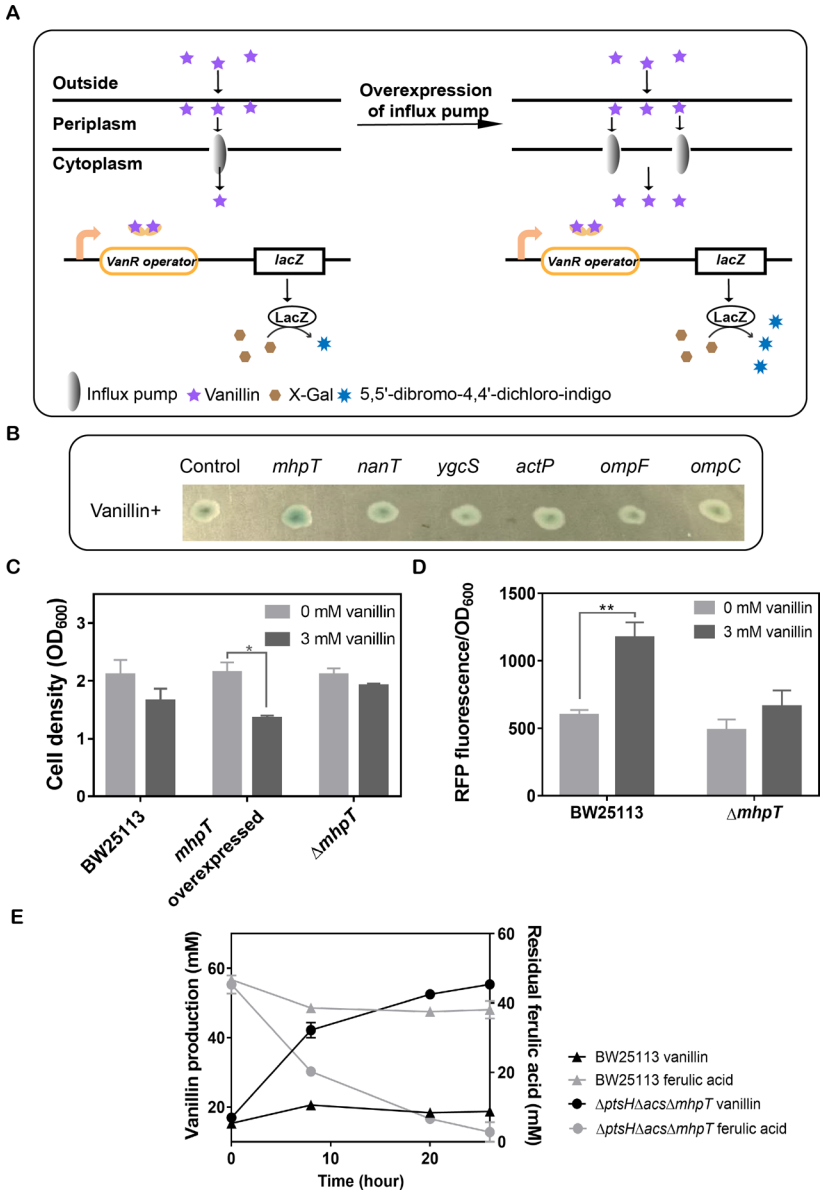

Figure 5. Whole-cell biosensor-aided influx pump screening. (A) Diagram showing the mechanism for influx pump screening. (B) Colonies of strain V3-4 overexpressing six membrane protein candidates were grown on agar plates supplemented with 3 mM vanillin and 30 μg/mL X-Gal. (C) Cell density of the indicated strains after treatment with 0 or 3 mM vanillin. (D) RFP fluorescence of strain BW25113 and Δ*mhpT* harboring plasmid pV3-4-RFP in the presence and absence of vanillin. (E) Time course profiles of vanillin production and residual ferulic acid accumulation in strain BW25113 or Δ*acs*Δ*ptsH*Δ*mhpT* (expressing the vanillin biosynthetic pathway). A total of 13.3 mM ferulic acid was supplemented five times at an interval of 1 h. The determination of time course began when all ferulic acid had been supplemented. The data shown are from three replicate experiments and are expressed as the mean ± SD. Two-tailed Student's *t* test was used for statistical analysis (*$P < 0.05$; **$P < 0.01$).

onate, sialic acid, sugar, and glycolate, respectively,[44−47] were selected to test whether these pumps transport vanillin. We also selected OmpF and OmpC to test vanillin flux through these channels. Constructs overexpressing these genes were selected from the *E. coli* ASKA library (A Complete Set of *E. coli* K-12 ORF Archive)[48] and individually introduced into strain V3-4. Among them, the strain overexpressing MhpT exhibited the darkest blue color (Figure 5B). To further explore the possible role of MhpT in vanillin transportation, the growth of strains with overexpressed or knocked-out MhpT was compared in the presence of extracellular vanillin. Vanillin impedes cell growth due to its toxicity (Figure S7).[49−52] When MhpT was overexpressed, the inhibitory effect of vanillin on cell growth increased in severity. In contrast, MhpT knockout rescued the cell growth inhibition caused by vanillin (Figure 5C). Next, our vanillin whole-cell biosensor was used to compare the intracellular vanillin concentrations of wild-type and Δ*mhpT* cells. The results revealed that the Δ*mhpT* cells displayed a significantly lower intracellular vanillin concentration (Figure 5D). These results suggest that MhpT may play an important role in vanillin influx.

Finally, we constructed strain Δ*acs*Δ*ptsH*Δ*mphT* and used this strain for vanillin biosynthesis. The time course of vanillin production and substrate consumption was compared between strain Δ*acs*Δ*ptsH*Δ*mphT* and wild-type BW25113. For the mutant strain, vanillin production reached 55.4 mM at 26 h with a yield of 90% (Figure 5E), which is the highest production from

https://dx.doi.org/10.1021/acs.jafc.0c07886
J. Agric. Food Chem. 2021, 69, 3114−3123

recombinant *E. coli* strains expressing the "*fcs-ech*" operon reported to date (Table S4).

DISCUSSION

This study extended the application of whole-cell biosensors to screening for efflux and influx pumps of small molecules on a whole genome scale, which will be critical in the construction of various natural product cell factories. The total vanillin production from the Δ*acrA* strain did not significantly improve. However, the inactivation of this protein significantly elevated the intracellular vanillin concentration, which was sensed by the whole-cell biosensor, demonstrating that the variation in vanillin transport triggered a biosensor response. Therefore, whole-cell biosensors can be applied to explore small-molecule transmembrane transport. First, our screening strategy can be simplified to select colonies from a random genome mutagenesis library under extracellular supplementation of specific compounds to identify genes involved in transmembrane transport. Mutant strains lacking an efflux pump would result in higher intracellular accumulation and more intense blue color. Next, influx pump proteins can be identified by screening a gene overexpression library under extracellular supplementation of specific compounds. Mutant strains overexpressing an influx pump will result in a higher intracellular accumulation. Following this strategy, MphT was identified as related to vanillin influx. This whole-cell biosensor-based strategy significantly accelerated the identification of transport-related genes in microbial genomes, and therefore, it should have applications in small-molecule transmembrane transport studies.

TRP-based whole-cell biosensors are powerful and effective for the optimization of vanillin cell factories. Although some vanillin-responsive TRPs have been reported,[22,53,54] their dynamic range and induction specificity are not sufficient for high-throughput screening applications. In this study, the VanR protein originally induced by vanillic acid[24] was engineered to respond specifically to vanillin but not to vanillic acid or vanillyl alcohol, revealing the power of directed evolution and plasticity of the ligand-binding pocket. For variant V3-4, approximately 13.7-fold VanR induction was attained from 0−9.5 mM vanillin. Replacing tyrosine at position 103 and arginine at position 148 with glycine and isoleucine, respectively, disrupted the hydrogen bond, and a salt bridge formed between the carboxyl group of vanillic acid and these two residues, thus abolishing vanillic acid induction. Discriminating vanillin (product) from the byproducts, vanillic acid, and vanillyl alcohol, using a biosensor, is important because the formation of these two byproducts would split the biosynthetic carbon flow and cause difficulties in downstream vanillin purification.[34,55] Therefore, biosensor quality definitely affects the composition of the biosynthetic products.

Directed genome evolution has proven effective in identifying novel genomic targets related to the efficiency of vanillin biosynthesis. The intracellular CoA pool is highly important for vanillin biosynthesis,[23] possibly limiting the first catalytic step. PEP accumulation,[36] caused by the inactivation of *ptsH*, leads to more efficient CoA regeneration from acetyl-CoA metabolism, causing the largest improvement in vanillin biosynthesis. Therefore, other strategies that increase the CoA pool *in vivo* should be beneficial for improving vanillin biosynthesis.

In conclusion, we developed a customized vanillin biosensor by engineering the VanR protein and used the biosensor as a high-throughput screening tool to facilitate directed genome evolution of a vanillin cell factory. Novel genomic targets involved in vanillin biosynthesis were successfully identified. Most importantly, the application of whole-cell biosensors was expanded to explore transmembrane transport-related proteins, which is a promising tool for the development of natural product cell factories and the transmembrane transport of target compounds.

Finally, combined with the strong screening capacity, directed genome evolution is an excellent alternative to targeted metabolic engineering strategies. The newly discovered genomic functions deduced from identified genomic targets will provide insights into microbial physiological and metabolic regulation.

ASSOCIATED CONTENT

Supporting Information

The Supporting Information is available free of charge at https://pubs.acs.org/doi/10.1021/acs.jafc.0c07886.

(Figure S1) Vanillin binding models of VanR variants, (Figure S2) positive correlation between LacZ activity and vanillin production from strain V3-4 harboring plasmids pBAD-EFG, (Figure S3) mutant strains selected from the random transposon insertion library, (Figure S4) determination of the insertion site of the transposon in the mutant strains by sequence, (Figure S5) vanillin production (normalized to cell density) of strain BW25113 with the indicated genes knocked out, (Figure S6) PEP and pyruvate regulate the forward and reverse Pta reactions comparison, (Figure S7) cell growth of strain BW25113 treated with different concentrations of vanillin at 37 °C for 8 h, (Table S1) strains and plasmids used in this study, (Table S2) primers used in this study, (Table S3) gene targets disrupted by the transposons were identified in randomly selected mutant strains from the transposon insertion library, and (Table S4) biotechnological production of vanillin from ferulic acid using recombinant strains (PDF)

AUTHOR INFORMATION

Corresponding Authors

Jian-Ming Jin − *Beijing Key Laboratory of Plant Resources Research and Development, Beijing Technology and Business University, Beijing 100048, China*; Phone: 86-10-68984917; Email: jinjianming@btbu.edu.cn

Wei Chen − *CAS Key Laboratory of Microbial Physiological and Metabolic Engineering, State Key Laboratory of Microbial Resources, Institute of Microbiology, Chinese Academy of Sciences, Beijing 100101, China; State Key Laboratory of Transducer Technology, Institute of Microbiology, Chinese Academy of Sciences, Beijing 100101, China*; Phone: 86-10-64806150; Email: chenw@im.ac.cn

Shuang-Yan Tang − *CAS Key Laboratory of Microbial Physiological and Metabolic Engineering, State Key Laboratory of Microbial Resources, Institute of Microbiology, Chinese Academy of Sciences, Beijing 100101, China*; orcid.org/0000-0002-1056-8690; Phone: 86-10-64806140; Email: tangsy@im.ac.cn

Authors

Xuanxuan Zhang − *CAS Key Laboratory of Microbial Physiological and Metabolic Engineering, State Key Laboratory of Microbial Resources, Institute of Microbiology, Chinese Academy of Sciences, Beijing 100101, China;*

https://dx.doi.org/10.1021/acs.jafc.0c07886
J. Agric. Food Chem. 2021, 69, 3114−3123

University of Chinese Academy of Sciences, Beijing 100049, China

Yang He − *School of Pharmacy, Chengdu University, Chengdu 610106, China*

Zhe Wu − *CAS Key Laboratory of Microbial Physiological and Metabolic Engineering, State Key Laboratory of Microbial Resources, Institute of Microbiology, Chinese Academy of Sciences, Beijing 100101, China*

Guoxia Liu − *CAS Key Laboratory of Microbial Physiological and Metabolic Engineering, State Key Laboratory of Microbial Resources, Institute of Microbiology, Chinese Academy of Sciences, Beijing 100101, China*

Yong Tao − *CAS Key Laboratory of Microbial Physiological and Metabolic Engineering, State Key Laboratory of Microbial Resources, Institute of Microbiology, Chinese Academy of Sciences, Beijing 100101, China*

Complete contact information is available at: https://pubs.acs.org/10.1021/acs.jafc.0c07886

Author Contributions

[#]X.X.Z. and Y.H. contributed equally to the work.

Author Contributions

S.-Y.T., W.C., and J-M.J. conceived the idea and supervised the research. X.X.Z. constructed the strains, plasmids, and libraries. X.X.Z. and W.C. did the whole-cell biosensor work. X.X.Z. and Z.W. did the screening of libraries and the HPLC analysis. Y.H. did molecular docking and related analysis. Y.T. contributed reagents/materials/analysis tools. Y.T. and Y.H. critically reviewed the manuscript. S.-Y.T., W.C., and J-M.J. performed data analysis and wrote the paper. All of the authors reviewed, approved, and contributed to the final version of the manuscript.

Funding

This work was supported by the National Key Research and Development Program of China (Grant 2018YFA0900701) and the National Natural Science Foundation of China (Grant Nos. 31971337, 31961133016, 31971382, and 31870072).

Notes

The authors declare no competing financial interest.

■ ACKNOWLEDGMENTS

We thank Dr. Junying Jia and Dr. Shuang Sun from Institute of Biophysics, Chinese Academy of Sciences for FACS screening.

■ ABBREVIATIONS

TRP, transcriptional regulatory protein; Fcs, feruloyl-CoA synthetase; Ech, feruloyl-CoA hydratase/aldolase; GltA, citrate synthase; TCA cycle, tricarboxylic acid cycle; RFP, red fluorescence protein; FACS, fluorescence-activated cell sorting; TAIL-PCR, thermal asymmetric interlaced PCR; HPLC, high-performance liquid chromatography; OD_{600}, optical density at a wavelength of 600 nm; PBS, phosphate buffered saline; X-Gal, 5-bromo-4-chloro-3-indolyl β-D-galactopyranoside; AD primers, arbitrary degenerate primers; FRT site, FLP recognition target site

■ REFERENCES

(1) Li, H.; Chen, W.; Jin, R.; Jin, J. M.; Tang, S. Y. Biosensor-aided high-throughput screening of hyper-producing cells for malonyl-CoA-derived products. *Microb. Cell Fact.* **2017**, *16*, 187.

(2) Siedler, S.; Stahlhut, S. G.; Malla, S.; Maury, J.; Neves, A. R. Novel biosensors based on flavonoid-responsive transcriptional regulators introduced into *Escherichia coli*. *Metab. Eng.* **2014**, *21*, 2−8.

(3) Tang, S. Y.; Fazelinia, H.; Cirino, P. C. AraC regulatory protein mutants with altered effector specificity. *J. Am. Chem. Soc.* **2008**, *130*, 5267−5271.

(4) Xiong, D.; Lu, S.; Wu, J.; Liang, C.; Wang, W.; Wang, W.; Jin, J. M.; Tang, S. Y. Improving key enzyme activity in phenylpropanoid pathway with a designed biosensor. *Metab. Eng.* **2017**, *40*, 115−123.

(5) Yao, J.; He, Y.; Su, N.; Bharath, S. R.; Tao, Y.; Jin, J.-M.; Chen, W.; Song, H.; Tang, S.-Y. Developing a highly efficient hydroxytyrosol whole-cell catalyst by de-bottlenecking rate-limiting steps. *Nat. Commun.* **2020**, *11*, 1515.

(6) Tang, S. Y.; Qian, S.; Akinterinwa, O.; Frei, C. S.; Gredell, J. A.; Cirino, P. C. Screening for enhanced triacetic acid lactone production by recombinant *Escherichia coli* expressing a designed triacetic acid lactone reporter. *J. Am. Chem. Soc.* **2013**, *135*, 10099−10103.

(7) Nielsen, J.; Keasling, J. D. Engineering Cellular Metabolism. *Cell* **2016**, *164*, 1185−1197.

(8) Li, M.; Xia, Q.; Zhang, H.; Zhang, R.; Yang, J. Metabolic engineering of different microbial hosts for lycopene production. *J. Agric. Food Chem.* **2020**, *68*, 14104−14122.

(9) Wu, J.; Chen, W.; Zhang, Y.; Zhang, X.; Jin, J. M.; Tang, S. Y. Metabolic engineering for improved curcumin biosynthesis in *Escherichia coli*. *J. Agric. Food Chem.* **2020**, *68*, 10772−10779.

(10) Zhang, C.; Chen, X.; Stephanopoulos, G.; Too, H. P. Efflux transporter engineering markedly improves amorphadiene production in *Escherichia coli*. *Biotechnol. Bioeng.* **2016**, *113*, 1755−1763.

(11) Chemler, J. A.; Fowler, Z. L.; McHugh, K. P.; Koffas, M. A. G. Improving NADPH availability for natural product biosynthesis in *Escherichia coli* by metabolic engineering. *Metab. Eng.* **2010**, *12*, 96−104.

(12) Zhao, J.; Li, Q.; Sun, T.; Zhu, X.; Xu, H.; Tang, J.; Zhang, X.; Ma, Y. Engineering central metabolic modules of *Escherichia coli* for improving β-carotene production. *Metab. Eng.* **2013**, *17*, 42−50.

(13) Kamminga, T.; Slagman, S.-J.; Bijlsma, J. J. E.; dos Santos, V. A. P. M.; Suarez-Diez, M.; Schaap, P. J. Metabolic modeling of energy balances in *Mycoplasma hyopneumoniae* shows that pyruvate addition increases growth rate. *Biotechnol. Bioeng.* **2017**, *114*, 2339−2347.

(14) Nyerges, A.; Csörgő, B.; Draskovits, G.; Kintses, B.; Szili, P.; Ferenc, G.; Revesz, T.; Ari, E.; Nagy, I.; Balint, B.; Vasárhelyi, B. M.; Bihari, P.; Számel, M.; Balogh, D.; Papp, H.; Kalapis, D.; Papp, B.; Pal, C. Directed evolution of multiple genomic loci allows the prediction of antibiotic resistance. *Proc. Natl. Acad. Sci. U. S. A.* **2018**, *115*, E5726−E5735.

(15) Walton, N. J.; Mayer, M. J.; Narbad, A. Inhibition of Quorum Sensing Mechanism and *Aeromonas hydrophila* Biofilm Formation by Vanillin. *Phytochemistry* **2003**, *63*, 505−515.

(16) Banerjee, G.; Chattopadhyay, P. Vanillin biotechnology: the perspectives and future. *J. Sci. Food Agric.* **2019**, *99*, 499−506.

(17) Gallage, N. J.; Møller, B. L. Vanillin-bioconversion and bioengineering of the most popular plant flavor and its *de novo* biosynthesis in the vanilla orchid. *Mol. Plant* **2015**, *8*, 40−57.

(18) Graf, N.; Altenbuchner, J. Genetic engineering of *Pseudomonas putida* KT2440 for rapid and high-yield production of vanillin from ferulic acid. *Appl. Microbiol. Biot.* **2014**, *98*, 137−149.

(19) Yoon, S. H.; Li, C.; Lee, Y. M.; Lee, S. H.; Kim, S. H.; Choi, M. S.; Seo, W. T.; Yang, J. K.; Kim, J. Y.; Kim, S. W. Production of vanillin from ferulic acid using recombinant strains of *Escherichia coli*. *Biotechnol. Bioproc. E.* **2005**, *10*, 378−384.

(20) Negishi, O.; Sugiura, K.; Negishi, Y. Biosynthesis of vanillin via ferulic acid in Vanilla planifolia. *J. Agric. Food Chem.* **2009**, *57*, 9956−9961.

(21) Overhage, J.; Priefert, H.; Steinbüchel, A. Biochemical and genetic analyses of ferulic acid catabolism in *Pseudomonas* sp. Strain HR199. *Appl. Environ. Microbiology* **1999**, *65*, 4837−4847.

(22) Liang, C.; Zhang, X.; Wu, J.; Mu, S.; Wu, Z.; Jin, J.-M.; Tang, S.-Y. Dynamic control of toxic natural product biosynthesis by an artificial regulatory circuit. *Metab. Eng.* **2020**, *57*, 239−246.

(23) Lee, E. G.; Yoon, S. H.; Das, A.; Lee, S. H.; Li, C.; Kim, J. Y.; Choi, M. S.; Oh, D. K.; Kim, S. W. Directing vanillin production from ferulic

acid by increased acetyl-CoA consumption in recombinant *Escherichia coli*. *Biotechnol. Bioeng.* **2009**, *102*, 200−208.
(24) Morabbi Heravi, K.; Lange, J.; Watzlawick, H.; Kalinowski, J.; Altenbuchner, J. Transcriptional regulation of the vanillate utilization genes (*vanABK* Operon) of *Corynebacterium glutamicum* by VanR, a PadR-like repressor. *J. Bacteriol.* **2015**, *197*, 959−972.
(25) Haldimann, A.; Wanner, B. L. Conditional-replication, integration, excision, and retrieval plasmid-host systems for gene structure-function studies of bacteria. *J. Bacteriol.* **2001**, *183*, 6384−6393.
(26) Liu, B.; Xiang, S.; Zhao, G.; Wang, B.; Ma, Y.; Liu, W.; Tao, Y. Efficient production of 3-hydroxypropionate from fatty acids feedstock in *Escherichia coli*. *Metab. Eng.* **2019**, *51*, 121−130.
(27) Bryksin, A.; Matsumura, I. Overlap extension PCR cloning. *Methods Mol. Biol.* **2013**, *1073*, 31−42.
(28) Miyazaki, K. MEGAWHOP cloning: a method of creating random mutagenesis libraries via megaprimer PCR of whole plasmids. *Methods Enzymol.* **2011**, *498*, 399−406.
(29) Lyskov, S.; Chou, F.-C.; Conchúir, S. Ó.; Der, B. S.; Drew, K.; Kuroda, D.; Xu, J. Q.; Weitzner, B. D.; Renfrew, P. D.; Sripakdeevong, P.; Borgo, B.; Havranek, J. J.; Kuhlman, B.; Kortemme, T.; Bonneau, R.; Gray, J. J.; Das, R. Serverification of molecular modeling applications: The Rosetta Online Server That Includes Everyone (ROSIE). *PLoS One* **2013**, *8*, No. e63906.
(30) Datsenko, K. A.; Wanner, B. L. One-step inactivation of chromosomal genes in *Escherichia coli* K-12 using PCR products. *Proc. Natl. Acad. Sci. U. S. A.* **2000**, *97*, 6640−6645.
(31) Li, H.; Liang, C.; Chen, W.; Jin, J.-M.; Tang, S.-Y.; Tao, Y. Monitoring in vivo metabolic flux with a designed whole-cell metabolite biosensor of shikimic acid. *Biosens. Bioelectron.* **2017**, *98*, 457−465.
(32) Liu, Y. G.; Whittier, R. F. Thermal asymmetric interlaced PCR: automatable amplification and sequencing of insert end fragments from P1 and YAC clones for chromosome walking. *Genomics* **1995**, *25*, 674−681.
(33) Merkens, H.; Beckers, G.; Wirtz, A.; Burkovski, A. Vanillate metabolism in *Corynebacterium glutamicum*. *Curr. Microbiol.* **2005**, *51*, 59−65.
(34) Converti, A.; Aliakbarian, B.; Domínguez, J. M.; Vázquez, G. B.; Perego, P. Microbial production of biovanillin. *Braz. J. Microbiol.* **2010**, *41*, 519−530.
(35) Priefert, H.; Rabenhorst, J.; Steinbüchel, A. Biotechnological production of vanillin. *Appl. Microbiol. Biotechnol.* **2001**, *56*, 296−314.
(36) Escalante, A.; Salinas Cervantes, A.; Gosset, G.; Bolívar, F. Current knowledge of the *Escherichia coli* phosphoenolpyruvate-carbohydrate phosphotransferase system: peculiarities of regulation and impact on growth and product formation. *Appl. Microbiol. Biotechnol.* **2012**, *94*, 1483−1494.
(37) Campos-Bermudez, V. A.; Bologna, F. P.; Andreo, C. S.; Drincovich, M. F. Functional dissection of *Escherichia coli* phosphotransacetylase structural domains and analysis of key compounds involved in activity regulation. *FEBS J.* **2010**, *277*, 1957−1966.
(38) Brown, T. D. K.; Jones-Mortimer, M. C.; Kornberg, H. L. The enzymic interconversion of acetate and acetyl-coenzyme A in *Escherichia coli*. *J. Gen. Microbiol.* **1977**, *102*, 327−336.
(39) Du, D.; Wang, Z.; James, N. R.; Voss, J. E.; Klimont, E.; Ohene-Agyei, T.; Venter, H.; Chiu, W.; Luisi, B. F. Structure of the AcrAB-TolC multidrug efflux pump. *Nature* **2014**, *509*, 512−515.
(40) Nishino, K.; Yamada, J.; Hirakawa, H.; Hirata, T.; Yamaguchi, A. Roles of TolC-dependent multidrug transporters of *Escherichia coli* in resistance to beta-lactams. *Antimicrob. Agents Chemother.* **2003**, *47*, 3030−3033.
(41) Nishino, K.; Yamaguchi, A. Analysis of a complete library of putative drug transporter genes in *Escherichia coli*. *J. Bacteriol.* **2001**, *183*, 5803−5812.
(42) Sulavik, M. C.; Houseweart, C.; Cramer, C.; Jiwani, N.; Murgolo, N.; Greene, J.; DiDomenico, B.; Shaw, K. J.; Miller, G. H.; Hare, R.; Shimer, G. Antibiotic susceptibility profiles of *Escherichia coli* strains lacking multidrug efflux pump genes. *Antimicrob. Agents Chemother.* **2001**, *45*, 1126−1136.
(43) Nikaido, H. Porins and specific channels of bacterial outer membranes. *Mol. Microbiol.* **1992**, *6*, 435−442.
(44) Ferrández, A.; Garciá, J. L.; Díaz, E. Genetic characterization and expression in heterologous hosts of the 3-(3-hydroxyphenyl) propionate catabolic pathway of *Escherichia coli* K-12. *J. Bacteriol.* **1997**, *179*, 2573−2581.
(45) Gimenez, R.; Nuñez, M. F.; Badia, J.; Aguilar, J.; Baldoma, L. The gene *yjcG*, cotranscribed with the gene *acs*, encodes an acetate permease in *Escherichia coli*. *J. Bacteriol.* **2003**, *185*, 6448−6455.
(46) Nilsson, I.; Prathapam, R.; Grove, K.; Lapointe, G.; Six, D. A. The sialic acid transporter NanT is necessary and sufficient for uptake of 3-deoxy-d-manno-oct-2-ulosonic acid (Kdo) and its azido analog in *Escherichia coli*. *Mol. Microbiol.* **2018**, *110*, 204−218.
(47) Pao, S. S.; Paulsen, I. T.; Saier, M. H., Jr. Major facilitator superfamily. *Microbiol. Mol. Biol. Rev.* **1998**, *62*, 1−34.
(48) Kitagawa, M.; Ara, T.; Arifuzzaman, M.; Ioka-Nakamichi, T.; Inamoto, E.; Toyonaga, H.; Mori, H. Complete set of ORF clones of *Escherichia coli* ASKA library (a complete set of *E. coli* K-12 ORF archive): unique resources for biological research. *DNA Res.* **2005**, *12*, 291−299.
(49) Luziatelli, F.; Brunetti, L.; Ficca, A. G.; Ruzzi, M. Maximizing the efficiency of vanillin production by biocatalyst enhancement and process optimization. *Front Bioeng. Biotechnol.* **2019**, *7*, 279.
(50) Fitzgerald, D. J.; Stratford, M.; Gasson, M. J.; Ueckert, J.; Bos, A.; Narbad, A. Mode of antimicrobial action of vanillin against *Escherichia coli*, *Lactobacillus plantarum* and *Listeria innocua*. *J. Appl. Microbiol.* **2004**, *97*, 104−113.
(51) Zaldivar, J.; Martinez, A.; Ingram, L. O. Effect of selected aldehydes on the growth and fermentation of ethanologenic *Escherichia coli*. *Biotechnol. Bioeng.* **1999**, *65*, 24−33.
(52) Yoon, S. H.; Lee, E. G.; Das, A.; Lee, S. H.; Li, C.; Ryu, H. K.; Choi, M. S.; Seo, W. T.; Kim, S. W. Enhanced vanillin production from recombinant *E. coli* using NTG mutagenesis and adsorbent resin. *Biotechnol. Prog.* **2007**, *23*, 1143−1148.
(53) Sana, B.; Chia, K. H. B.; Raghavan, S. S.; Ramalingam, B.; Nagarajan, N.; Seayad, J.; Ghadessy, F. J. Development of a genetically programed vanillin-sensing bacterium for high-throughput screening of lignin-degrading enzyme libraries. *Biotechnol. Biofuels* **2017**, *10*, 32.
(54) de los Santos, E. L. C.; Meyerowitz, J. T.; Mayo, S. L.; Murray, R. M. Engineering transcriptional regulator effector specificity using computational design and *in vitro* rapid prototyping: developing a vanillin sensor. *ACS Synth. Biol.* **2016**, *5*, 287−295.
(55) Perez-Rodriguez, N.; Oliveira, R. P. D.; Agrasar, A. M. T.; Dominguez, J. M. Ferulic acid transformation into the main vanilla aroma compounds by *Amycolatopsis* sp ATCC 39116. *Appl. Microbiol. Biotechnol.* **2016**, *100*, 1677−1689.

https://dx.doi.org/10.1021/acs.jafc.0c07886
J. Agric. Food Chem. 2021, 69, 3114−3123